Kumar and Kumar *Earth, Planets and Space* (2018) 70:29
https://doi.org/10.1186/s40623-018-0794-8

Earth, Planets and Space

FULL PAPER

Open Access

Solar flare effects on D-region ionosphere using VLF measurements during low- and high-solar activity phases of solar cycle 24

Abhikesh Kumar* and Sushil Kumar

Abstract

The effects of solar flares on the propagation of subionospheric VLF signals from NWC and NLK transmitter stations monitored at a low-latitude station, Suva (18.2°S, 178.4°E), Fiji, between December 2006 and December 2010 (an unprecedented solar minimum of solar cycles 23 and 24) and between January 2012 and December 2013 (moderate solar activity at the peak of solar cycle 24) have been analyzed to find solar flare time D-region changes. The amplitude and phase enhancements associated with solar flares were observed in the signals from both stations which are due to an increase in the electron density of the D-region as a result of extra ionization caused by the solar flares. The solar flare-induced perturbations in both the amplitude and phase of VLF signals were used to determine D-region ionospheric parameters: H' (the ionospheric reflection height) and β (rate of increase in electron density with height) using Long Wave Propagation Capability (LWPC) version 2.1 modeling. A comparative analysis of the ionospheric D-region parameter changes carried out for this location shows a greater increase in β and decrease in H' during low-solar activity period than during moderate-solar activity period, for the same class of flares. Our results also show greater differences in the values of β and H' for strong flares in comparison with weak flares under both low- and moderate-solar activity conditions.

Keywords: Solar flares, VLF perturbations, D-region ionosphere, Solar activity

Introduction

Solar flares, mainly having X-ray wavelengths of the order of tenths of nanometers, permeate the D-region of the ionosphere and enhance the electron density by extra ionization (e.g., Mitra 1974). The D-region, acting as a reflecting layer, is important for long-wave communication and navigation systems. The very low-frequency (VLF, 3–30 kHz) radio waves generated by strong lightning discharges and navigational transmitters propagate through the waveguide bounded by the Earth's surface and the lower ionosphere (D-region), known as the Earth–ionosphere waveguide (EIWG) with relatively low attenuation of about 2–3 dB/Mm (Davies 1990, p. 367). Under normal conditions in the absence of solar flares, D-region ionization is mainly produced by the Sun's Lyman-α radiation. During solar flares, the X-ray flux from the sun increases considerably, which penetrates to the D-region and increases the electron density via extra ionization of the neutral constituents, particularly nitrogen and oxygen.

McRae and Thomson (2004) studied the ionospheric D-region parameter changes, H' and β, as a function of solar X-ray flux by using solar flare-induced perturbations to the VLF amplitude and phase of the Omega, NPM (USA) and NLK (USA) signals received at Dunedin, New Zealand. H' is a measure of the ionospheric reference height in kilometer and β is the electron density sharpness in km^{-1} of the D-region. McRae and Thomson (2004), using the Long Wave Propagation Capability

*Correspondence: kumar_ab@usp.ac.fj
School of Engineering and Physics, Faculty of Science, Technology and Environment, The University of the South Pacific, Suva, Fiji

(LWPC) and ModeFinder computer codes, established that during solar flare-associated D-region ionization, H' decreases in proportion to the logarithm of the X-ray flux intensity. They found that the typical reduction in H' can be from a midday unperturbed value of about 71 km to about 58 km for an $X5$ class solar flare; β can increase from 0.39 km^{-1} to a saturation level of about 0.52 km^{-1}. Thomson et al. (2004, 2005) found that the phase perturbations for X class solar flares to NDK (USA), NLK, NPM and Omega (Australia) signals recorded at Dunedin were more closely correlated with the X-ray flux than was the amplitude. From the measurements of the GQD (Anthorn, UK, 22.1 kHz) transmitter signal at Belgrade, Grubor et al. (2005) found that flares of C to X classes perturbed subionospheric VLF signals during a period of low-solar activity period between 2004 and 2005. Raulin et al. (2006) studied solar flares using VLF sudden phase anomalies (SPAs) on NDAK (North Dakota, USA, 13.1 kHz), HAI (Haiku, USA, 13.6 kHz) and ARG (12.9 kHz) transmitter signals received at Atibaia (ATI), Brazil. Their results suggest that the occurrence of SPAs due to weak solar flares, of class C and below, was higher during solar minima, but the occurrence of SPAs was not dependent on the solar activity for stronger class flares. Recently, Tan et al. (2014) studied the effects of 26 solar flare, of classes $C2.6$ to $X3.2$, on the amplitude of the NWC (Australia) signal recorded at a low-latitude site at Tay Nguyen University, Vietnam. They found that during the solar flares, β increased from 0.3 to 0.506 km^{-1}, while H' decreased from 74 to 60 km.

In this study, the effects of solar flares during two time periods on the amplitude and phase of subionospheric VLF signals from NWC (19.8 kHz) and NLK (24.8 kHz) monitored at Suva (18.1°S, 178.4°E), Fiji, a low-latitude station in the South Pacific region, were analyzed. The first time interval was from December 2006 to December 2010, a period during the unprecedented solar minimum of solar cycles 23 and 24 (low solar activity, $Rz = 9$); the second was from January 2012 to December 2013, a period at the peak of solar cycle 24 (moderate solar activity, $Rz = 60$). The NWC–Suva path is in an almost east–west direction, whereas the NLK–Suva is in a northeast–southwest direction. These two paths have been selected to cover a larger time zone and hence to observe the effect of a greater number of solar flares. The signal perturbations due to A and B class flares are masked by background noise (signal variation), so we considered only C, M and X flares. A comparison was made between the VLF perturbations associated with the same classes of solar flares during both low and moderate levels of solar activity. During the prolonged solar minimum period (2006–2010), the ionosphere shrank to its lowest level (Heelis et al. 2009; Liu et al. 2011), which enabled us to study the low-latitude D-region response to space weather. A greater number of solar flare-associated VLF perturbations were observed during this interval due to the extended time frame and the increased sensitivity of the D-region to solar flares during solar minima. The solar flare-associated signal amplitude and phase enhancements of varying flare intensities and any dependence of the effects of solar flares on solar activity were investigated. Selected VLF perturbation events associated with solar flares for a wide range of flare classes were modeled using LWPC version 2.1 to determine the effect of solar activity on the D-region changes associated with solar flares. The research reported above presented the variations in H' and β with respect to solar flare power for either low, mid- or high levels of solar activity separately. In the current study, the relationship between flare power and changes in H' and β is presented using an extensive amount of flare data (6 years) during both low- and moderate (peak of the current solar cycle)-solar activity conditions and a comparison is made between them.

Experimental data and analysis

A software-based VLF amplitude and phase logger, known as 'SoftPAL' for short, was used to log the VLF signals that are minimum shift key (MSK)-modulated (Dowden and Adams 2008; Kumar et al. 2008). The VLF signals were continuously recorded with a time resolution of 0.1 s against GPS-based time. From the 0.1 s resolution data, 1-min-averaged values of amplitude and phase were obtained and used to display the amplitude and phase perturbations associated with solar flares. The transmitter–receiver great circle paths (TRGCPs) of the NWC and NLK transmitter signals to Suva are presented in Fig. 1. For different classes of flares, any relationship between the amplitude or phase perturbations

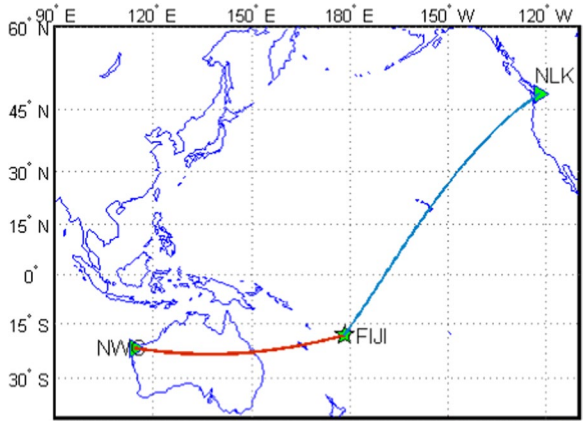

Fig. 1 Map showing the transmitters and receiver (Suva, Fiji) sites and their TRGCPs

against solar flare power, and the variations in the H' and β parameters were analyzed for the VLF signals when their propagation paths were in the daylight region. The XL band X-ray fluxes from the GOES satellites, which are found to vary proportionally in both time and level of observed VLF perturbation, were also utilized. The X-ray fluxes were recorded in two wavelength bands: (1) 0.05–0.4 nm referred to as 'short' or 'XS' and (2) 0.1–0.8 nm, referred to as 'long' or 'XL,' by the X-ray imager aboard the GOES satellite. Solar flares are classified in different categories, namely *A*, *B*, *C*, *M* and *X* in the 'XL' band, based on the peak flux intensities (in W/m^2). In this study, solar flux data in the 'XL' band were obtained from http://www.swpc.noaa.gov/ftpmenu/warehouse.html. The XL band has greater fluxes and is used in the *C*, *M* and *X* flare classifications. It also produces measurable D-region conductivity changes associated with class *C* and above flares. In this paper, we do not intend to study the effects of *A* and *B* class flares on VLF. At the time of writing, for GOES satellites (GOES 10 and 12), the XL band fluxes saturate at about *X*17, whereas the XS fluxes saturate at about *X*8 (Thomson et al. 2005), making them unsuitable for the study of VLF perturbations associated with stronger flares.

The number of daytime solar flares that occurred during the periods of data analysis is given in Table 1. *C*, *M* and *X* class flares were only considered as these mainly produced noticeable effects on the VLF signals. Along with the count of solar flares, the yearly mean values of the sunspot numbers are also given. It is evident that *C* class flares occurred most often, *M* class less frequently and *X* class least often. *X* class flares occurred only during December 2006 and for the years 2012 and 2013. Table 1 also indicates that the occurrence rate of solar flares depends on solar activity. The monthly mean value of amplitude ($A_{\text{background}}$) at the time of solar flare activity was subtracted from the value of peak amplitude during solar flare (A_{peak}) to determine the solar flare-induced perturbations in amplitude (ΔA), i.e., $\Delta A = A_{\text{peak}} - A_{\text{background}}$, which is similar to the method used by Todoroki et al. (2007). An equivalent method was used to obtain the phase perturbation, which is given as $\Delta\phi = \phi_{\text{peak}} - \phi_{\text{background}}$, where ϕ_{peak} is the value of peak phase during solar flare and $\phi_{\text{background}}$ is the phase just before the occurrence of a flare. The ΔA and $\Delta\phi$ values were thus estimated from the SoftPAL plots manually for all the flares on NLK and NWC. The threshold values of $\Delta A = 0.2$ dB and $\Delta\phi = 2^{o}$ were taken to confirm the influence of a solar flare. For modeling the D-region parameters, we inspected the pre-solar flare background X-ray flux for many events and it was found that during *C* and higher-class flares, the background flare level (in the XL band) remains very low in comparison with the flare time flux, e.g., for a *C*1.5 flare, the background flux was 1.6×10^{-7} W/m^2, while that at the peak of the perturbation was 1.5×10^{-6} W/m^2, which is approximately one order of magnitude higher. For these flares, we subtracted the background flux density from the flux density at the peak of the flare. Thus, for most of the daytime flares for *C* class and above, the VLF signatures were quite clearly identified and correlated with the peak flux density. The amplitude and phase perturbations were not observed for all the daytime flares, particularly those which were of weak class (weak *C* and below), or for which the background flux was sufficiently high.

Table 1 Occurrence of solar flares of different classes (*C*, *M*, *X*) as observed by GOES for the periods of data analysis (*low solar activity, **moderate solar activity) together with the average sunspot numbers for each year

Months	Average sunspot no. (R_z)	Number of flares		
		C	*M*	*X*
*December 2006	13.6	53	5	4
*January 2007–December 2007	7.5	72	10	0
*January 2008–December 2008	2.9	13	2	0
*January 2009–December 2009	3.1	5	0	0
*January 2010–December 2010	16.5	54	10	0
**January 2012–December 2012	57.7	680	70	6
**January 2013–December 2013	64.9	671	47	8
Total		1548	144	18

Results

Solar flare effects on subionospheric VLF propagation

All the solar flare-induced VLF perturbations displayed enhancements in amplitude and phase. The effects of solar flares on VLF signals were only observed when a portion of the TRGCPs were under daylight conditions. Figures 2 and 3 present several cases of solar flare-induced VLF perturbations on amplitude and phase (where available) on July 05, 2012, and May 13, 2013, wherein the variation of solar flux measured by GOES satellite in the XL band is also shown. The consistent variation of amplitude and phase with solar flux indicates that XL band radiation is well correlated with extra D-region ionization during solar flares.

Solar flares on July 05, 2012

A series of solar flare events, recorded by GOES satellites, perturbed the amplitude and phase of the NWC signal on July 05, 2012. The variation of X-ray flux during the seven flare events of classes *M*1.1, *M*2.5, *M*1.0, *C*7.1, *M*2.3, *M*4.7 and *C*9.1, together with the amplitude and phase of the NWC signal, is shown in Fig. 2a, b. During the time in which these flares occurred, 00–05 h UT

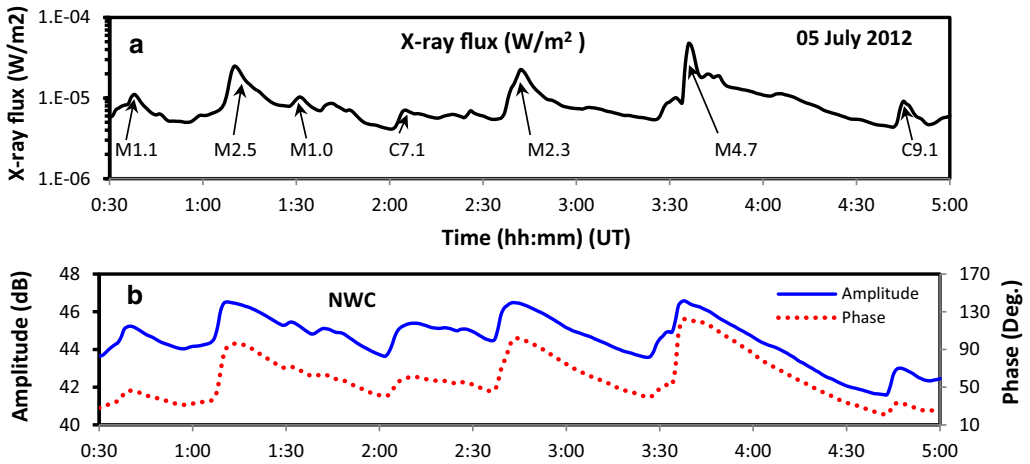

Fig. 2 **a** Variations in the GOES X-ray flux in W/m^2 during the solar flares of July 05, 2012. **b** Variations in the amplitude and phase of the NWC signal during the July 05, 2012, solar flares

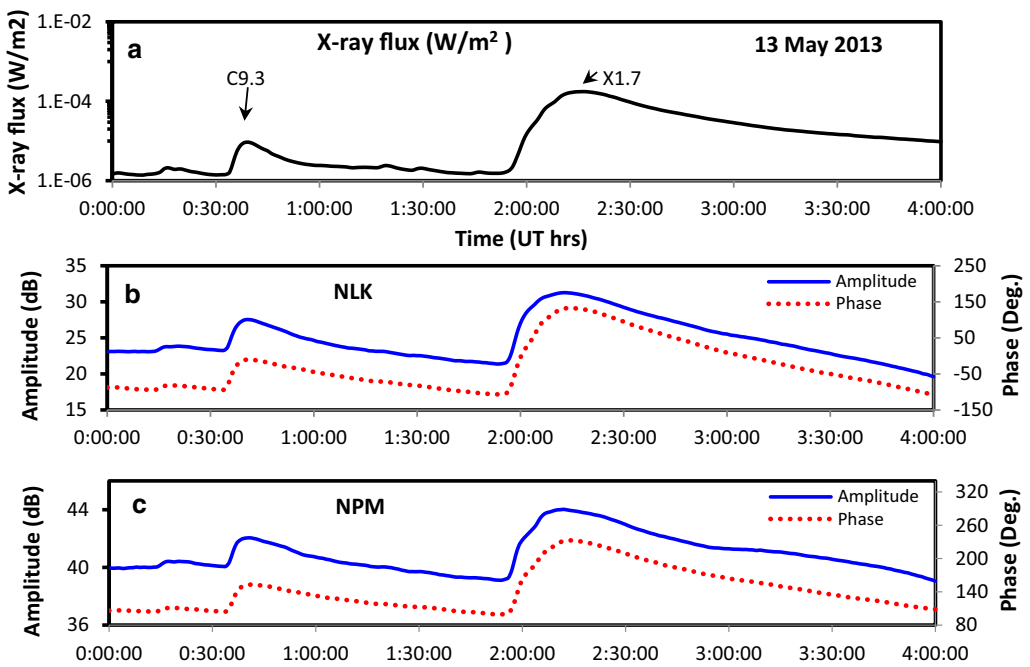

Fig. 3 **a** Variations in the GOES X-ray flux in W/m^2 during the solar flares of May 13, 2013. **b**, **c** Variations in the amplitude and phase of the NLK and NPM signals during the May 13, 2013 solar flares

(12–17 h LT), the NWC to Suva TRGCP was completely in daylight. The NLK signal was off-air, so no effect could be observed in it. During these flares, the NWC amplitude and phase enhancements showed clear proportional variation with the X-ray flux intensity. The ΔA values for NWC ranged from 1.4 dB (*C*7.1) to 2.6 dB (*M*4.7) for these seven flares, while $\Delta\phi$ ranged from 12° to 54°. Throughout this period, the signal strength remained above the normal daytime value because the next flare occurred before the amplitude recovered fully. The peaks of the amplitude and phase of the signal appear to be well aligned with the peak of the X-ray flux during all the flares. However, upon close observation, time delays (Δt) between amplitude and phase peaks with the X-ray

peak ranging from 0.5 to 5 min were estimated for some of these flares, with the *C*7.1 flare revealing the largest time delay of 5 min. Δt is an important quantity that can be used to study the ionospheric response to the flares (Zigman et al. 2007); however, it is not the subject of this study.

Solar flares on May 13, 2013

The effects of two solar flares of classes *C*9.3 and *X*1.7 that occurred on May 13, 2013, were observed on the phase and amplitude of the NLK and NPM signals simultaneously. The *C*9.3 flare began at 0:32 UT and finished at 0:46 UT, while the *X*9.0 flare started at 01:53 UT and ended at 02:32 UT. The NWC signal was inactive; hence, no effect was seen on it. The variations in the X-ray flux together with the NLK and NPM amplitude and phase during both the flares are shown in Fig. 3a–c. For the *C*9.3 flare, values of ΔA and $\Delta\phi$ of 4.2 dB and 82° and 1.9 dB and 49° were measured for the NLK and NPM signals, respectively. Likewise, values of ΔA and $\Delta\phi$ of 9.8 dB and 220° and 4.8 dB and 133° were measured for the NLK and NPM signals, respectively, for the *X*1.7 flare. From these data, it can be seen that for the same flare, different signals are perturbed to different extents: In this case, NLK demonstrates stronger perturbations to amplitude and phase than the NPM signal. A zero time delay (Δt) was observed for the *C*9.3 flare, with the amplitude and phase peaks for both signals occurring at the same time as the solar flare flux peak. The *X*1.7 flare, however, showed a Δt of about − 3.5 min between the peaks of flux and amplitude, with the amplitude peak occurring before the flare flux peak. However, the peaks of the phase and the flux are in line showing zero Δt between them for both of the signals. (The NPM amplitude and phase data are used here only once to illustrate simultaneous observations of the solar flare-associated perturbations on VLF; we have not used the NPM signal for any further analysis.)

Effects of solar activity on solar flare-induced VLF perturbations

Of all the flares listed in Table 1, measurable effects of 50 flares were observed on signals from NLK and of 34 flares on NWC signals during the period of low solar activity (December 2006 to December 2010). Similarly, during the period of moderate solar activity (2012–2013), the effects of 137 flares were seen on NLK and of 127 flares on NWC signals. VLF perturbations might not be observed during daylight hours, for all the flares, because either the VLF transmitters were off (or no data were available) or weaker flares of class *C* and below may not have produced any detectable VLF perturbations. The ΔA associated with solar flares for NLK and NWC during the periods December 2006–2010 and 2012–2013 has been plotted as a function of X-ray solar flare power as shown in Fig. 4. The flares utilized were from classes *C*1.0 to *X*6.5 and happened when the signal TRGCPs were in complete daylight. The complete daylight paths for NWC and NLK to Suva correspond to 22:00 UT–05:00 UT (next day) and 18:00 UT–01:00 UT, respectively. The $\Delta\phi$ variation with respect to the peak flare power for the two signals is shown Fig. 5. The level of $\Delta\phi$ is quite similar for both the signals, with NLK showing a maximum of up to 200° and NWC showing a maximum of up to 150°. The main conclusion from these observations is that during low solar activity, a number of weak flares, with flare power 0–5 dB, showed correspondingly weak phase perturbations. However, during a period of moderate solar activity, very few flares showed measurable phase perturbations below the 5 dB flare power, with none below 2 dB. The fit curves of Figs. 4 and 5 are polynomial (order 3) and their linear regression coefficients (r) are indicated, which are significantly above 0.8.

To investigate dependence of ΔA and $\Delta\phi$ on solar zenith angle (SZA), we selected flares occupying a narrow category range (*M*1.0–*M*1.3) but covering a wide range of SZA that affected the NLK signal. The plots of ΔA and $\Delta\phi$ against SZA in Fig. 6 show that ΔA and $\Delta\phi$ depend upon (decrease with) SZA, particularly for SZA > 40°, which is consistent with a recent study by Bouderba et al. (2016). $\Delta\phi$ is better correlated with SZA than ΔA, as indicated by linear regression coefficient (r) values of 0.754 for $\Delta\phi$ and 0.663 for ΔA against SZA.

D-region modeling for solar flare effects: Wait parameters

VLF signal perturbations due to solar flares during the studied low- and moderate-solar activity periods, measured both on the amplitude and phase of NLK and NWC signals, were used to determine the accompanying changes in D-region parameters (H' in km and β in km^{-1}) using the LWPC (version 2.1) code. Since the daytime D-region is SZA dependent and the values of H' and β are different in LWPC-created segments along the paths, it is not possible to find a single undisturbed value of H' and β along the entire path. Because of this difficulty, values of H' and β are estimated at the mid-location of TRGCPs (e.g., McRae and Thomson 2000), with respect to which the changes in D-region parameters due to solar flares are obtained by using LWPC modeling.

The initial step for determining the variations in H' and β with flare power was to establish the unperturbed values of H' and β for which SZA values for mid-TRGCP paths of the VLF signals at the times of flare occurrence were calculated. The SZA was calculated by the Web site service of http://www.solartopo.com/solar-orbit.htm and unperturbed H' and β were calculated using the relationships between SZA and D-region parameters given by

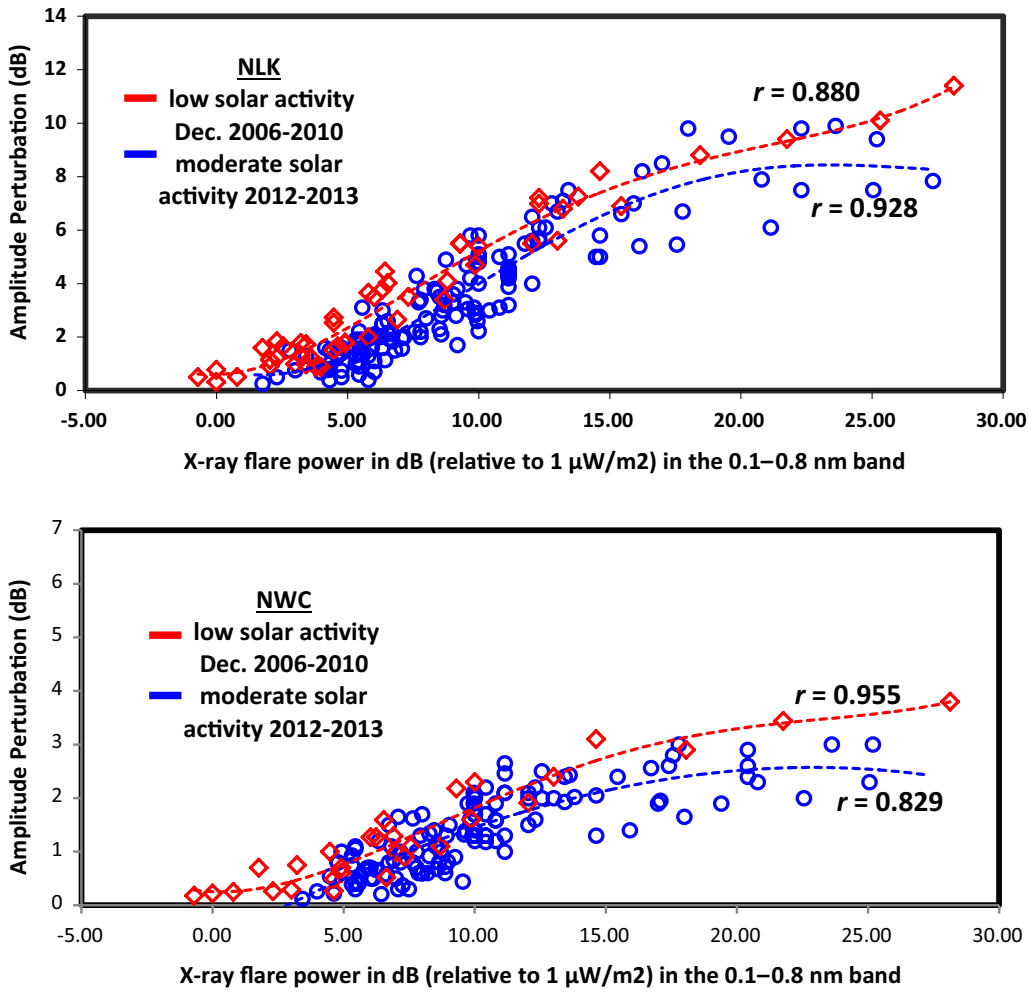

Fig. 4 VLF amplitude perturbations for NLK and NWC measured at Suva, Fiji, as function of solar flare X-ray flux measured in dB relative to 1 μW/m^2 in the 0.1–0.8 nm band, for low-solar activity conditions (red points and corresponding red best-fit curve) and moderate-solar activity conditions (blue points and corresponding blue best-fit curve)

McRae and Thomson (2000) for low solar activity and by Thomson (1993) for high solar activity. To investigate the solar activity dependence of solar flare-associated D-region changes, we selected flares that occurred within the SZA $-$ 40° $< \chi <$ 40°. This essentially minimizes the SZA effect (as shown in Fig. 6) on solar flare-induced VLF perturbations, and hence, D-region changes. The level of perturbations for a narrow range of flare flux intensities (e.g., *C*3.0–*C*3.9) was further investigated within this SZA range and it was found that no apparent variation existed with the varying SZA.

The perturbed values of ionospheric H' and β during solar flares were obtained by varying the values of H' and β so as to match the observed perturbed amplitude ($A + \Delta A$) and phase ($\phi + \Delta\phi$). This was done by adjusting the values of H' (at intervals of 0.05 km) and β (at intervals of 0.001 km^{-1}). To obtain the observed values of the amplitude and phase, the RANGE model was run using the EXPONENTIAL substring (rexp) in the LWPC. A range of amplitudes and phases were generated as text files for various segments, starting from the transmitter leading to the receiver. In this way, the observed amplitude and phase at the receiver are obtained. In some cases, it was not possible to find the exact match for both the observed amplitude and phase. In such circumstances, H' and β were varied to obtain the closest values of observed perturbed amplitude and perturbed phase. The values of H' and β during solar flares were modeled considering the values at mid-path location as ambient values along the entire TRGCP, which is a robust approximation that has also been used in earlier research (e.g., McRae and Thomson 2000).

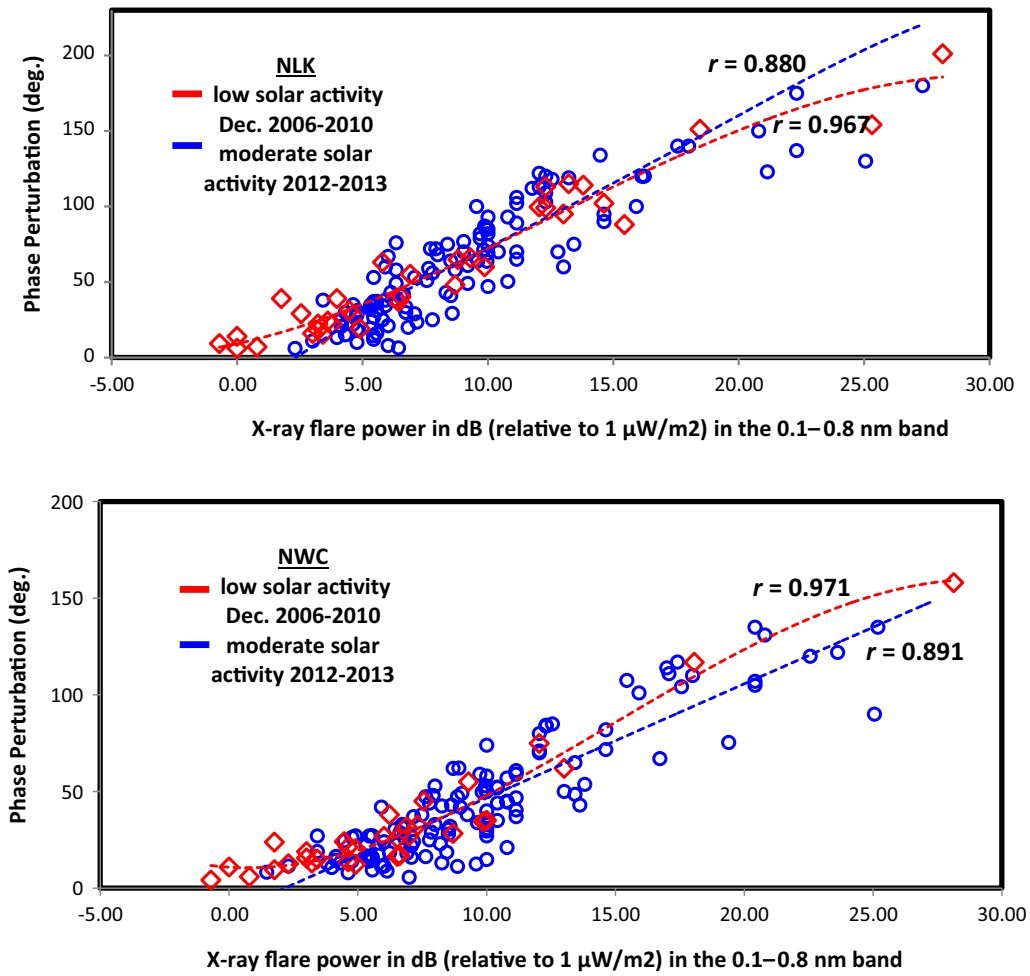

Fig. 5 VLF phase perturbations for NLK and NWC measured at Suva, Fiji, as functions of solar flare X-ray flux measured in dB relative to 1 µW/m^2 in the 0.1–0.8 nm band, for low-solar activity conditions (red points and corresponding red best-fit curves) and moderate-solar activity conditions (blue points and corresponding blue best-fit curves)

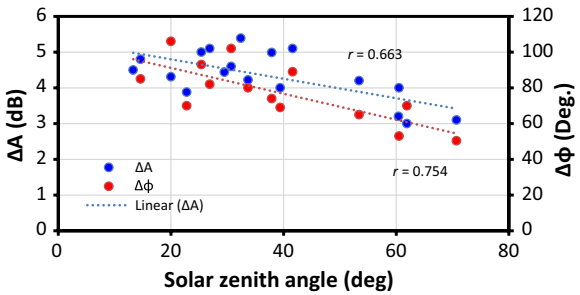

Fig. 6 Variation of amplitude and phase perturbations to the NLK signal against the absolute values of solar zenith angle for flares occurring in the narrow range of class *M*1.0–*M*1.3

To model the D-region ionosphere during solar flares, 12–15 solar flare events were selected that caused both amplitude and phase perturbations during each of the low- and moderate-solar activity periods. These are the flares that lie nearest to the best-fit curves for the amplitude perturbation versus the X-ray flare power of Fig. 4 and phase perturbation versus flare power of Fig. 5. This was done to minimize the error in estimating H' and β due to variations of ΔA and $\Delta\phi$ for any solar flare away from the best-fit curves. The variations of H' and β for these flares of varying intensity, ranging from weak (*C*1.0) to strong (*X*6.5) classes, are plotted in Fig. 7 for the NLK and NWC signals as functions of solar flare power during

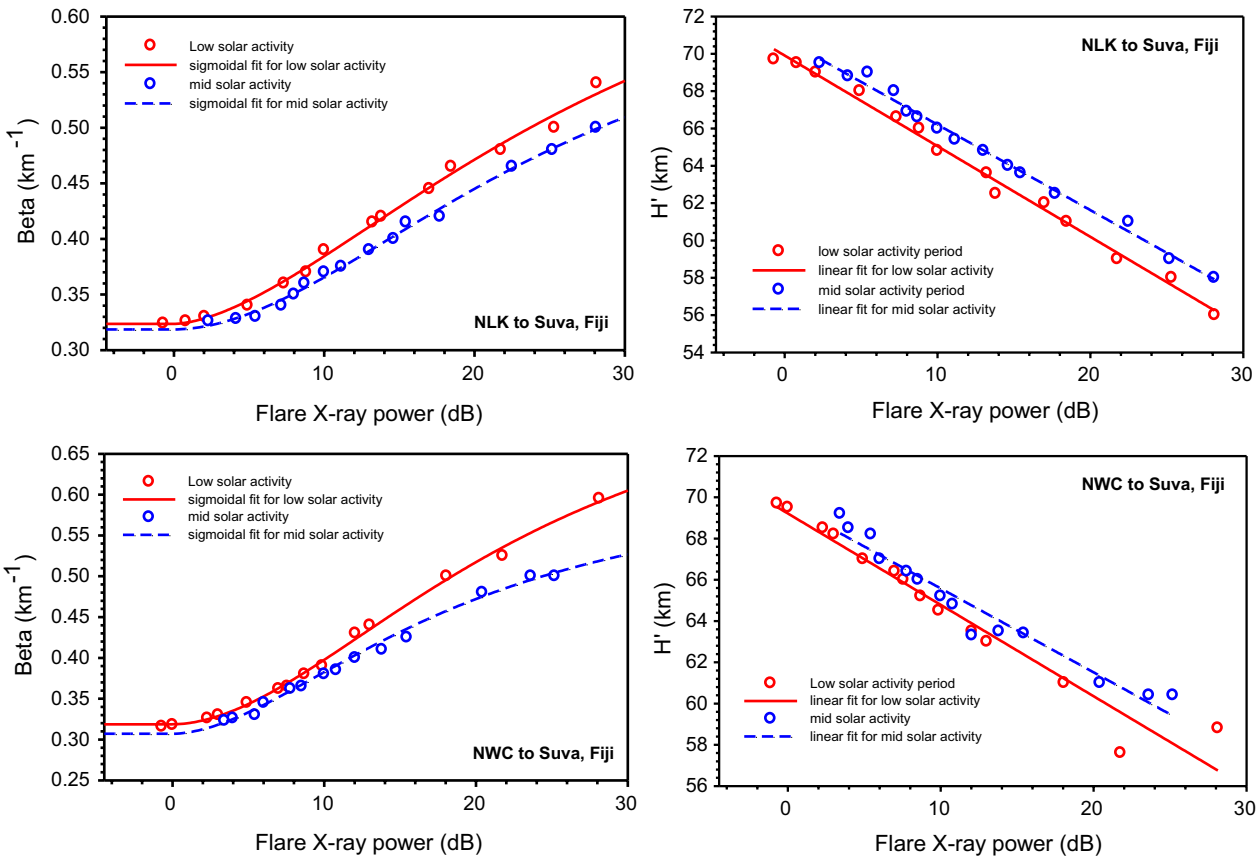

Fig. 7 Ionospheric D-region parameters H' and β, found as functions of solar X-ray flare power from the VLF amplitude and phase perturbations of NLK and NWC signals received at Suva during the periods of low- and mid-level (moderate) solar activity. The red points and best-fit lines correspond to low-level solar activity, while the blue points and best-fit lines correspond to mid-level (moderate) solar activity periods

the low- and moderate-solar activity conditions. Sigmoid curves were used to plot the best-fit graphs for β, while a linear fit was found to be most appropriate for H'. β, as seen from the panels on the left-hand side of Fig. 7, shows a sigmoidal variation, increasing quite linearly with respect to the flare power in the range 5–20 dB for the NLK and NWC signals during low- and moderate-solar activity periods. Below 5 dB, the fit curves for both signals flatten approaching a minimum β of approximately 0.32 km^{-1}, while they become less steep above 20 dB but do not flatten completely. A distinct difference in β, of about 0.04 km^{-1} for the same class of flares, was observed during periods of low and moderate solar activity, when β was found to be higher and lower, respectively. This difference in the level of β is found to be more pronounced for intense M and X class flares than for weak C class flares.

The panels on the right-hand side of Fig. 7 show that H' decreases in direct proportion to the increasing logarithm of the X-ray flux. H' drops to between 56 km for the strong X6.5 flare and 70–71 km for weak C1.0 class flares from normal typical daytime value of about 70.7 km. Classes C1.0 and X6.5 correspond to 0 and 28 dB flare power, respectively. An interesting feature of the variation in H' with X-ray flux is that there is a difference in the reduction in H' for the same class of solar flares depending on the level of solar activity. For both signals, it was observed that H' decreases more during the low-solar activity period than during high-solar activity conditions for the same class of flares, as is evident from the gap separating the best-fit lines of H' versus flare power in Fig. 7. For the NLK and NWC signals, H' is estimated to decrease by approximately 1 km more during low levels of solar activity than during moderate levels for strong solar flares of similar class.

We adopted an alternative approach to make the scientific method more rigorous and to ensure that Fig. 7 shows all of the flare events, and not just a subset of 12–15 data points (i.e., to remove any bias in Fig. 7). Average values of the change in amplitude and phase for discrete flare powers were obtained for selected bins, e.g., the average value of the ΔA and $\Delta\phi$ was obtained for all

the data points between flare powers 0 and 4.9 dB. In a similar manner, the averaged phase and amplitude results within specific X-ray flare power bins (0–4.9, 5–9.9, 10–14.9, 15–19.9 and 20–25 dB) were obtained, and a new set of graphs for ΔA and $\Delta\phi$ for the two signals are plotted in Fig. 8 with appropriate best-fit lines. Based on the standard deviation of the points from the mean value, the standard error was calculated and included in the graphs of ΔA and $\Delta\phi$. Using the mean values of ΔA and $\Delta\phi$ for each flare power bin, LWPC code was run to determine H' and β and the results are plotted in Fig. 9. The relationship of β and H' versus the flare power essentially resembles the same form as that in Fig. 7, but as pointed out, it now includes the effects of all the solar flare events on each signal. During periods of low solar activity, the statistical reliability of the effects of solar flares above 15 dB is poorer than for those below 15 dB due to the relative scarcity of data points. Further study with a larger data set, particularly above 15 dB, will give better insight into Wait parameters for solar flares.

During a solar flare, H' changes (decreases) to a perturbed value, H'_p. Hence, the difference $\Delta H' = H' - H'_p$ is proportional to the amplitude and phase change, for daytime propagation. To study the sensitivity of the lower ionosphere to the solar activity conditions, it is very important to compare the quantity $\Delta H'$ during the two solar activity periods. In order to do this, the graphs of $\Delta H'$ versus flare power for the three signals are plotted as

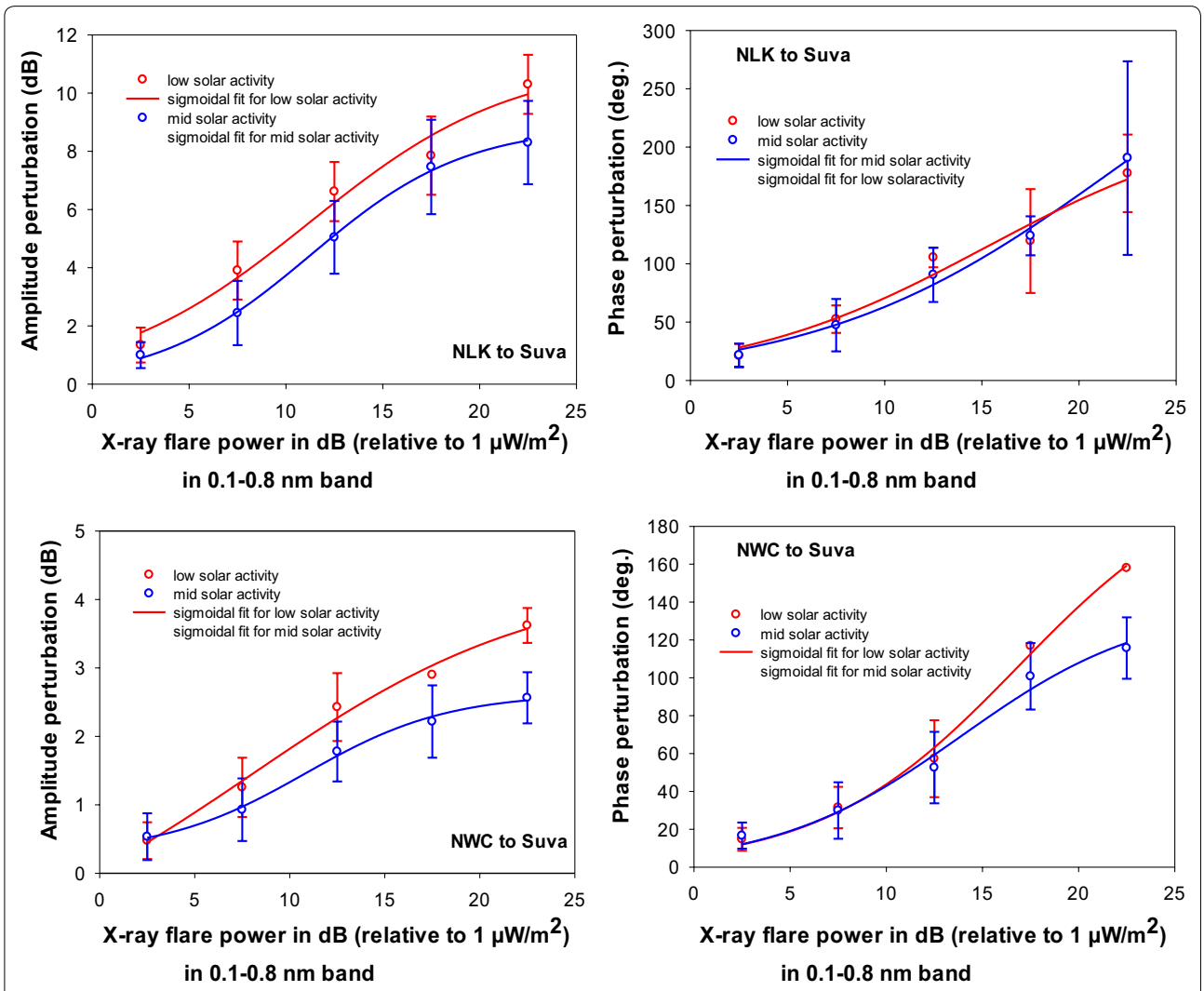

Fig. 8 Average VLF amplitude and phase perturbations of selected flare power bins for NLK and NWC as functions of solar flare X-ray flux measured in dB relative to 1 μW/m^2 in the 0.1–0.8 nm band, for low-solar activity conditions (red points and corresponding red best-fit curves) and moderate-solar activity conditions (blue points and corresponding blue best-fit curves)

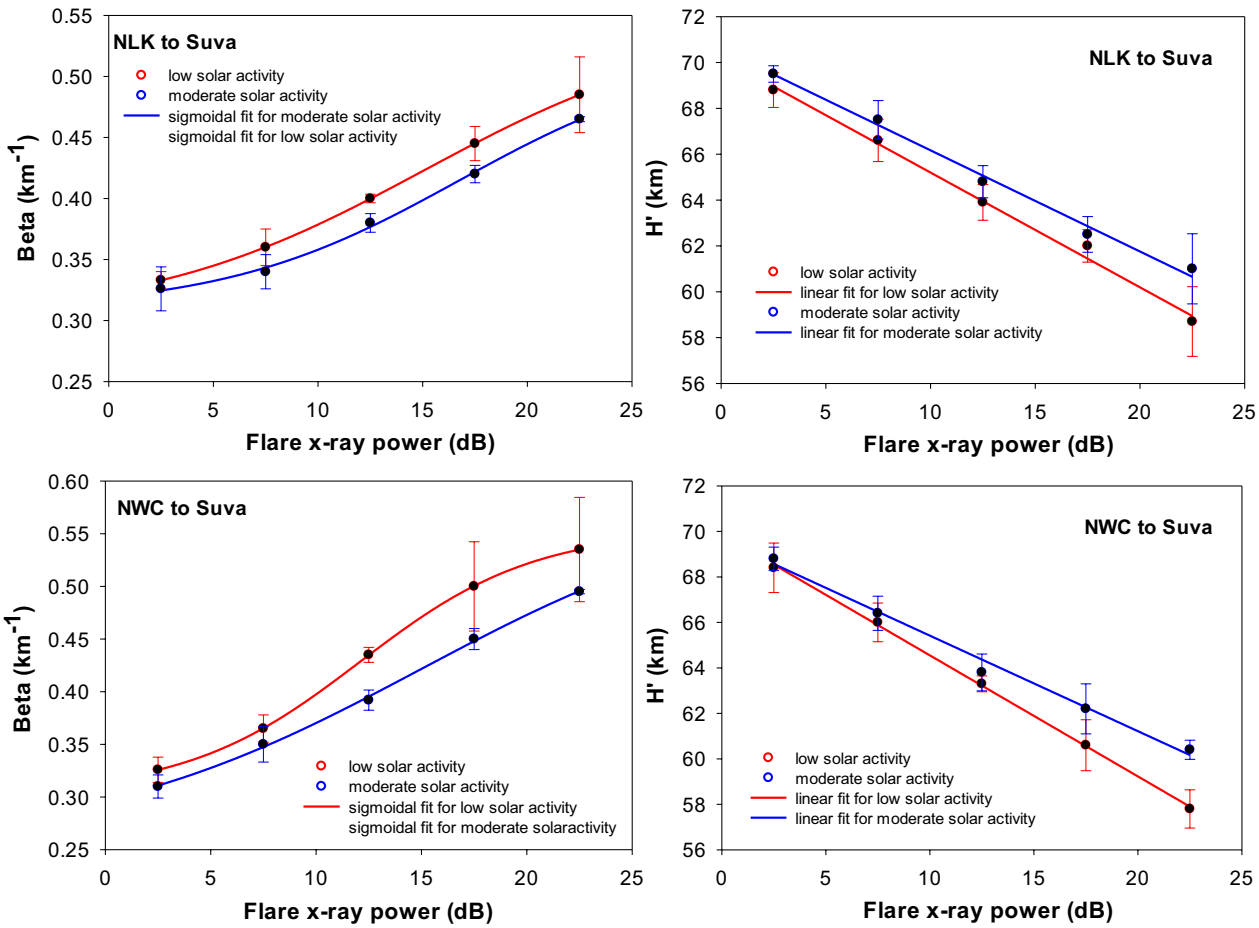

Fig. 9 Ionospheric D-region parameters H' and β, determined as functions of solar X-ray flare power from the mean VLF amplitude and phase perturbations of selected flare power bins of Fig. 8 during the low- and moderate-solar activity periods. The points plotted in red and their best-fit lines correspond to low solar activity, while the points plotted in blue and their best-fit lines correspond to moderate-solar activity periods

shown in Fig. 10. The plots reveal that $\Delta H'$ increases linearly with increasing flare strength. But most importantly, $\Delta H'$ is about 2 km greater for strong X class flares during low-solar activity periods than during the moderate-solar activity period.

The D-region electron density height profiles, $N_e(h)$ in cm^{-3}, for our position were constructed using the Wait profile and are valid up to about 100 km altitude (Wait and Spies 1964), following $N_e(h) = 1.43 \times 10^7$ [exp $(-0.15H')$ exp $[(\beta - 0.15)(h - H')]$. We used the modeling results of the $M1.0$ solar flare events that occurred on February 08, 2010 (solar minimum), at 21:23 UT (09:23 LT) and on November 27, 2012 (moderate solar activity), at 21:26 UT (09:26 LT) and appeared in the NLK signal to investigate how the electron density profiles changed during solar flares in different solar activity periods. Both these flares occurred within the SZA $-\ 40° < \chi < 40°$. The unperturbed values of H' and β obtained from the LWPC modeling were 74.0 km and 0.325 km^{-1}, respectively. For the $M1.0$ flare during the solar minimum, the perturbed H' and β were 64.80 $\pm$ 0.05 km and 0.390 $\pm$ 0.001 km^{-1}, while for the $M1.0$ flare during moderate solar activity, the perturbed H' and β were 66.00 $\pm$ 0.05 km and 0.370 $\pm$ 0.001 km^{-1}. $N_e(h)$ in the altitude range of 50–90 km for both perturbed (red and blue dashed lines) and unperturbed (black solid line) values of the Wait parameters are shown in Fig. 11. $N_e(h)$ is comparably larger for the solar flare-induced D-region ionosphere than during normal conditions, which accounts for the increase in the amplitude of the signals. In addition, from our analysis of Fig. 11, it can be observed that the enhancement in $N_e(h)$ for the same class of flares during the solar minimum is greater than during moderate levels of solar activity, which could be another reason why β increases and H' decreases more during solar minima than during periods of moderate solar activity. Figure 11 shows that for a $M1.0$ class flare and a typical

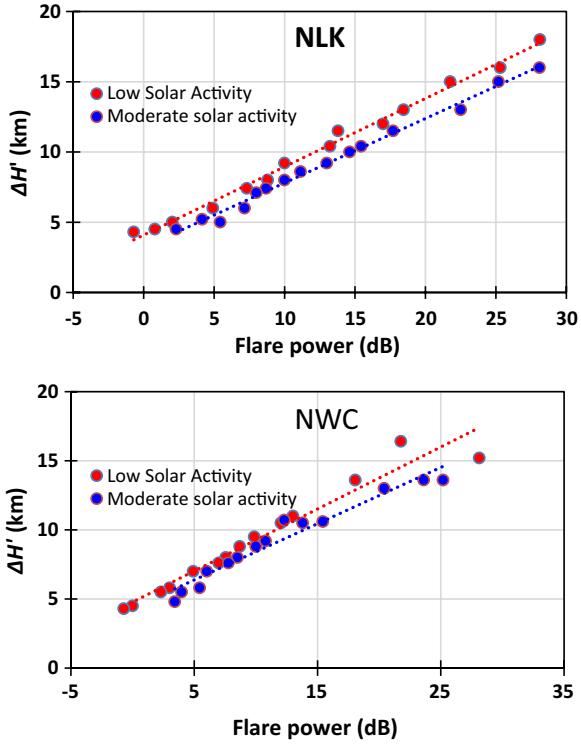

Fig. 10 $\Delta H'$ versus flare power for the two signal paths during periods of low and moderate solar activity. $\Delta H' = H' - H'_p$, where H' is the quiescent-level ionospheric reflection height and H'_p is the reflection height during the solar flare peak

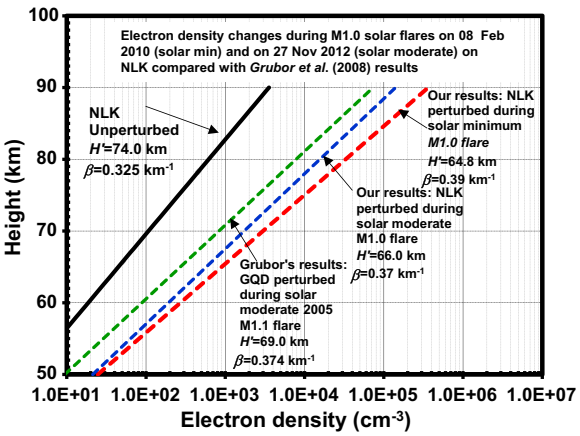

Fig. 11 Electron densities determined by LWPC VLF modeling during the *M*1.0 solar flare of February 08, 2010 (red dashed line—solar minimum), and of November 27, 2012 (blue dashed line—moderate solar activity), compared with normal unperturbed electron densities (solid black line) for NLK to Suva path. Also shown is comparison of electron density plot of Grubor et al. (2008) results (green dashed line) for an *M*1.1 flare during a period of moderate solar activity

daytime ionospheric height of 74 k, N_e is 7815 cm^{-3} for the solar minimum compared to 4170 cm^{-3} for moderate solar activity. A comparison of our results with those of Grubor et al. (2008) for an *M*1.1 flare which affected the GQD to Belgrade path on July 12, 2005 (moderate solar activity), at 12:59 UT demonstrates an N_e value of 2038 cm^{-3} at a height of 74 km, which was much lower than the level during the solar minimum. Hence, it is evident from our results and from comparison with those of Grubor et al. (2008) that the enhancement of N_e during a solar minimum is greater than during moderate or maximum levels of solar activity for the same class of flares.

Discussion

The effects of solar flares on subionospheric VLF propagation during low- and moderate-solar activity periods showed enhancements in the amplitude and phase, which were found to be higher during periods of low solar activity than during the period of high solar activity in this study. The solar flare-induced signal enhancement can be explained in terms of electron density enhancements (Grubor et al. 2005) through which propagating VLF signals get reflected from a sharper and lower D-region ionospheric boundary penetrating less into the D-region, and hence undergo less attenuation/absorption than under normal unperturbed conditions. This is consistent with our results in Figs. 2 and 3, where the VLF phase and amplitude always increased during solar flares. But Kolarski and Grubor (2014), based on the amplitude and the phase perturbation of the 22.1 kHz GQD signal trace from Skelton (54.72°N, 2.88°W) to Belgrade (44.85°N, 20.38°E), reported that the pattern of signal perturbation is not always the same for solar flares. They found that for some flares the amplitude and phase delay increased, while for others, the perturbations in amplitude showed a short-duration decrease followed by an increase and a decrease in the phase delay. They stated that solar flares affected the VLF wave propagation in the EIWG by changing the lower ionosphere electron density height profile differently for different solar flare events. Bouderba et al. (2016), using the solar flare-induced perturbations of the VLF signal from the NRK transmitter (37.5 kHz, 63.85°N, 22.45°W) received at Algiers (RALG: 36.7°N, 03.13°E) with a TRGCP of 3495 km and LWPC modeling, calculated the change in the attenuation coefficient and fading displacement and suggested that the sign (negative or positive) of the perturbed signal parameters depends on the propagating distance. Šulic et al. (2016) from the analysis of amplitude and phase data received at Belgrade from four European transmitters during a seven-year period (2008–2014) found a range

of amplitude and phase perturbations that varied for different paths. Also, their statistical results showed that the size of amplitude and phase perturbations to the VLF/LF radio signal was correlated with the intensity of the X-ray flux. However, these authors did not state the exact relationship using fit curves between the level of VLF perturbation and the flare flux intensity.

A distinct difference seen between the ΔA and flare power curves for the two signals (Fig. 4) is the level of perturbations for similar class flares during the low- and moderate-solar cycle periods. The solar flares of similar class demonstrate higher levels of ΔA values during periods of low solar activity than during the period of moderate solar activity for both signals. A maximum difference in ΔA of up to 0.5 dB for the NLK and NWC signals is seen at a flare power level of approximately 15 dB. The solar flares of strength $C1.0$ to $C1.3$ during the period of low solar activity produced perturbations, whereas flares of same class did not produce any detectable perturbations during the period of moderate solar activity, which is due to the higher sensitivity of the D-region during low solar activity.

The best-fit curves for ΔA versus the flare power for the VLF signals are similar in form to those obtained earlier by McRae and Thomson (2004), Thomson et al. (2005) and more recently by Kumar and Kumar (2014). However, variation between ΔA and the flux intensity during solar flares for the two paths shows that the level of amplitude perturbation is higher for the NLK signal (24.8 kHz, maximum of ~ 11.5 dB) and lower for the NWC signal (19.8 kHz, ~ 3.5 dB). Similar results were obtained by McRae and Thomson (2004) using NLK and NPM transmission to Dunedin. Their results showed NLK displaying ΔA of up to 8 dB, while for NPM, ΔA of up to 4 dB for the same flares was recorded. The authors indicated that the VLF amplitude perturbation level of different signals is frequency dependent. At higher frequencies, the signals exhibit greater amplitude perturbation compared to lower frequencies for the same flares. This increase in amplitude enhancement as a function of frequency was attributed to the second-order TM mode (McRae and Thomson 2004) which becomes comparable to that of the first-order TM mode at the receiver. This dissimilarity in the amplitude perturbation levels could also depend upon the path orientation of NWC and NLK for the same flares because the directions in which the flares are directed and the solar flux to which they are subjected could be different for separate paths. One of the paths could be under more solar radiation (different solar zenith angles) than the other; hence, it may be more susceptible to solar flare-induced perturbations. Unlike the ΔA curves, the $\Delta\phi$ curves are similar in form and level of perturbation for the two signals (Fig. 5) during both the low- and moderate-solar activity periods. Thus, it is seen that ΔA is the main measurable quantity that can distinguish the solar flare effects on VLF during different levels of solar activity and not $\Delta\phi$; however, measurements of both the quantities are essential to accurately model the D-region to determine its flare time parameters H' and β.

Using LWPC simulation, McRae and Thomson (2004) estimated a decrease in H' of 12 km and an increase in β of 0.13 km^{-1} relative to their normal daytime values for an $X3.0$ class flare on the NLK to Dunedin, New Zealand, path. For another class $X5$ flare for this path, they estimated a 13 km decrease in H' and the same increase in β. Recently, Kumar et al. (2015) estimated a decrease of 9.4 km in H' and an increase of 0.126 km^{-1} in β for an $X1.5$ class flare on the NPM–Suva path. According to Thomson et al. (2005), the D-region could be used as a solar flare strength indicator for flares greater than class $X17$ (for which the GOES detector saturates) up to $X45$ by extrapolating the phase profile.

During solar flares, β increases, which causes an increase in VLF signal amplitudes for paths such as those of NLK and NWC to Suva. According to Thomson and Clilverd (2001), ionization at the lower altitudes (50–65 km) as a result of galactic cosmic rays (e.g., Rishbeth and Garriott 1969), apart from the solar Lyman-α radiation, also contributes to this increase in β. This effect is intensified near solar minima (when compared with solar maximum) by the slightly lower solar Lyman-α flux and enhanced galactic cosmic rays at low latitudes (Thomson and Clilverd 2000), which is the reason why the increase in β is greater for low solar activity than for moderate solar activity for same class flares, as shown by our analysis. If the flare is strong enough to produce extra ionization above a certain threshold of Lyman-α and galactic cosmic rays, the value of β will not increase further, i.e., it will display a saturation effect similar to that of the NWC signal for the period of moderate solar activity, as shown in Fig. 7.

The relationship between the changes in the D-region, H' and β, and the flare power during solar flares of varying intensities has been reported by a number of researchers (e.g., Thomson and Clilverd 2001; McRae and Thomson 2004; Thomson et al. 2005; Tan et al. 2014). A nearly linear reduction of H' against the logarithm of flare flux was obtained for weak $C1$ up to strong $X45$ class flares. β was found to display sigmoidal variation with respect to flare power. The results presented here show similar variations of H' and β for the two long VLF paths. The authors above have presented the variations in H' and β with respect to solar flare power for either low, mid- or high solar activities separately. But in

this study, the relationship between the flare power and the changes in the ionospheric D-region H' and β have been presented using a comparative analysis during low- and moderate-solar activity conditions at a low-latitude station.

A distinct difference in the variation of H' and β with respect to the flare power is seen during the low- and moderate-solar activity periods. In general, the increase in β is found to be greater for low solar than moderate solar activity for similar class flares. The β value is estimated to be higher by about 0.04 km^{-1} for the same class of flares during low-solar activity period than during moderate-solar activity period for the two VLF signals. In addition, H' seems to be reduced further during the low-solar activity period (i.e., ~ 1–2 km) than the moderate-solar activity conditions for same class of flares. This can be clearly seen from the graphs of $\Delta H'$ versus flare power in Fig. 10. This difference in the level of β and H' is found to be more pronounced for strong M and X class flares than for low C class flares.

McRae and Thomson (2004) showed estimated plots of H' and β for low-, mid- and high-solar activity conditions. Their estimates were based on the assumption that for a given flare size, such as $M3$, same amount of X-ray flux is produced in any solar cycle and hence essentially the same total D-region ionization at any time. Thus, their plots revealed that for strong flares, especially X class, the β values were the same during all solar cycle conditions, while their H' values were also seen to be same for any class of solar flares. Their plots showed the difference at C and weak M class flares, where β was found to be significantly higher during high-solar activity and lower during low-solar activity conditions. For example, it is estimated from the plots of McRae and Thomson (2004) for solar flares around 4 dB strength (equivalent to $C2.5$ class); the β values were 0.39 km^{-1} for solar minimum and 0.41 km^{-1} for moderate solar activity. In contrast, our results indicate greater β values for the solar minimum than for the period of moderate solar activity for the same strength of flares, i.e., 0.35 km^{-1} and 0.33 km^{-1}, respectively. The results presented here imply greater differences in β and H' for stronger classes of solar flares during low- and moderate-solar activity conditions. Pacini and Raulin (2006) also investigated the relation between VLF sudden phase anomalies (SPAs) and solar X-ray flares to investigate whether it has a dependence on solar activity cycles. They found a significant correlation between the level of amplitude perturbation and the X-ray flux, F_X (time-integrated photon fluxes), in the range 0.5–2.0 Å. They showed that the amplitude perturbation versus F_X relation differs depending on the epoch within the solar cycle. Their results showed that for a given strength solar flare, $\Delta H'$ will be approximately 1 km greater during the solar minimum period than during the solar maximum, which is in agreement with our findings. These authors, however, did not study the variation of β for different solar activity cycles.

Summary and conclusions

The effects of solar flares during the unprecedented solar minimum of solar cycles 23 and 24 and the moderate-solar activity level ($Rz = 60$) during the maximum of solar cycle 24 on subionospheric VLF signals from NLK and NWC transmitters recorded at Suva, Fiji, reveals a clear dependence on solar activity. Both the amplitude and phase of VLF signals exhibited perturbations (enhancements) due to increased ionization from the solar flares that lowers H' and increases β of the lower edge of the D-region. Based on the results, the following conclusions are reached:

1. The solar flare-associated enhancements on both the amplitude and phase of VLF signals were found to vary proportionally with the logarithm of the X-ray flux. A comparison between the amplitude enhancements (ΔA) and the flux intensity for the two paths showed that ΔA is greater for the NLK signal (maximum of ~ 11.5 dB) and less for the NWC signal (~ 3.5 dB).
2. Solar flares of similar class produced higher values of ΔA during low solar activity than during periods of moderate solar activity. The level of phase perturbations is quite similar during low and moderate solar activities for all the signals, with NLK recording a maximum of up to 200° and NWC showing a maximum of up to 150°.
3. The solar flares lower the effective reflection height (H') by creating increased ionization (ref Fig. 11) that is approximately proportional to the logarithm of the X-ray flare flux intensity. The lower-edge ionospheric D-region sharpness (β) also increases significantly showing a sigmoidal variation with the logarithm of X-ray flare intensity.
4. A distinct difference in the variation of H' and β with respect to the flare power is seen during the low- and moderate-solar activity periods. In general, the increase in β is found to be greater for low solar activity than for moderate solar activity for similar class flares. In addition, the reduction in H' ($\Delta H'$) is greater by ~ 1–2 km during the period of low solar activity than during the period of moderate-solar activity conditions for same class of flares. This difference in the level of β and H' is found to be more pronounced for strong M and X class flares than for low C class flares.

Thus, it can be inferred that strong flares, especially *M* and *X* class, can increase the D-region electron density and the redistribution of electron density with height more during low-solar activity conditions, lowering the D-region ionosphere when it is very sensitive, than during higher-solar activity periods.

Authors' contributions
The author AK analyzed the VLF data for solar flares in consultation with SK. The manuscript was jointly prepared by AK and SK. Both authors read and approved the final manuscript.

Acknowledgements
The authors sincerely thank the Research Committee of the Faculty of Science, Technology and Environment, University of the South Pacific (USP), for initial financial support to carry out this work. The authors are also thankful to financial support by USP's main research office under the Strategic Research Theme (Grant No. 6177-3107-Acct-617704) under which a part of work has been carried out. Solar flux data were obtained from http://www.swpc.noaa.gov/ftpmenu/warehouse.html, and subionospheric VLF transmitter data are available from the first author.

Competing interests
The authors declare that they have no competing interests.

Publisher's Note

Received: 4 August 2017 Accepted: 30 January 2018
Published online: 12 February 2018

References

Bouderba Y, NaitAmor S, Tribeche M (2016) Study of the solar flares effect on VLF radio signal propagating along NRK-ALG path using LWPC code. J Geophys Res 121:6799–6807. https://doi.org/10.1002/2015JA022233
Davies K (1990) Ionospheric radio. Peregrinus, London
Dowden RL, Adams CDD (2008) SoftPAL. In: Proceedings of the 3rd VERSIM workshop, Tihany, Hungary, 15–20 Sept
Grubor D, Šulic D, Zigman V (2005) Influence of solar X-ray flares on the Earth-ionosphere waveguide. Serbian Astron J 171:29–35
Grubor D, Šulic D, Zigman V (2008) Classification of X-ray solar flares regarding their effects on the lower ionosphere electron density profile. Ann Geophys 26:1731–1740
Heelis RA, Coley WR, Burrell AG, Hairston MR, Earle GD, Perdue MD, Power RA, Harmon LL, Holt BJ, Lippincott CR (2009) Behavior of O^+/H^+ transition height during extreme solar minimum of 2008. Geophys Res Lett (USA) 36:L00C03. https://doi.org/10.1019/2009gl038652
Kolarski A, Grubor D (2014) Sensing the Earth's low ionosphere during solar flares using VLF signals and GOES solar X-ray data. Adv Space Res 53:1595–1602
Kumar A, Kumar S (2014) Space weather effects on the low latitude D-region ionosphere during solar minimum. Earth Planets Space 66(1):76. https://doi.org/10.1186/1880-5981-66-76
Kumar S, Kumar A, Rodger CJ (2008) Subionospheric early VLF perturbations observed at Suva: VLF detection of red sprites in the day. J Geophys Res 113:A03311. https://doi.org/10.1029/2007JA012734
Kumar S, Kumar A, Menk F, Maurya AK, Singh R (2015) Response of the low latitude D-region ionosphere to extreme space weather event of 14–16 December 2006. J Geophys Res Space Phys 120:788–799. https://doi.org/10.1002/2014JA020751
Liu L, Chen Y, Le H, Kurkin VI, Polekh NM, Lee CC (2011) The ionosphere under extremely prolonged low solar activity. J Geophys Res 116:A04320. https://doi.org/10.1029/2010JA016296
McRae WM, Thomson NR (2000) VLF phase and amplitude: daytime ionospheric parameters. J Atmos Sol Terr Phys 62(7):609–618
McRae WM, Thomson NR (2004) Solar flare induced ionospheric D-region enhancements from VLF phase and amplitude observations. J Atmos Sol Terr Phys 66:77–87
Mitra AP (1974) Ionospheric effects of solar flares. D. Reidel Publishing Company, Dordrecht
Pacini AA, Raulin J-P (2006) Solar X-ray flares and ionospheric sudden phase anomalies relationship: A solar cycle phase dependence. J Geophys Res 111:A09301. https://doi.org/10.1029/2006JA011613
Raulin J-P, Pacini AA, Kaufmann P, Correia E, Martinez MAG (2006) On the detectability of solar X-ray flares using very low frequency sudden phase anomalies. J Atmos Sol Terr Phys 68:1029–1035. https://doi.org/10.1016/j.jastp
Rishbeth H, Garriott OK (1969) Introduction to ionospheric physics. Academic Press, New York
Šulic DM, Sreckovic VA, Mihajlov AA (2016) A study of VLF signals variations associated with the changes of ionization level in the D-region in consequence of solar conditions. Adv Space Res 57(4):1029–1043. https://doi.org/10.1016/j.asr.2015.12.025
Tan LM, Thu NN, Ha TQ, Mourbouti M (2014) Solar flare induced D-region ionosphere changes using VLF amplitude observations at a low latitude side. Indian J Radio Space Phys 43:197–204
Thomson NR (1993) Experimental daytime VLF ionospheric parameters. J Atmos Sol Terr Phys 55:173–184
Thomson NR, Clilverd MA (2000) Solar cycle changes in daytime VLF subionospheric attenuation. J Atmos Sol Terr Phys 62(7):601–608
Thomson NR, Clilverd MA (2001) Solar flare induced ionospheric D-region enhancements from VLF amplitude observations. J Atmos Sol Terr Phys 63:1729–1737
Thomson NR, Rodger CJ, Dowden RL (2004) Ionosphere gives size of greatest solar flares. Geophys Res Lett 31:L06803
Thomson NR, Rodger CJ, Clilverd MA (2005) Large solar flares and their ionospheric D region enhancements. J Geophys Res 110:A06306
Todoroki Y, Maekawa S, Yamauchi T, Horie T, Hayakawa M (2007) Solar flare induced D region perturbation in the ionosphere, as revealed from a short-distance VLF propagation path. Geophys Res Lett 34:L03103
Wait JR, Spies KP (1964) Characteristics of the earth-ionosphere waveguide for VLF radio waves. Technical Note 300, National Bureau of Standards, Boulder, Colorado
Zigman V, Grubor D, Sulic D (2007) D-region electron density evaluated from VLF amplitude time delay during X-ray solar flares. J Atmos Sol Terr Phys 69:775–792